Electrochemical and thermal properties of SmBa0.5Sr0.5Co2O5þd cathode impregnated with Ce0.8Sm0.2O1.9 nanoparticles for intermediate- temperature solid oxide fuel cells

by Subardi -

Submission date: 22-Mar-2023 06:47PM (UTC-0700)
Submission ID: 2044036008
File name: Jurnal_ke_7_SBSC55_Infiltrated_SDC.pdf (2.02M)
Word count: 5505
Character count: 27769

INTERNATIONAL JOURNAL OF HYDROGEN ENERGY 42 (2017) 24338–24346

Available online at www.sciencedirect.com

ScienceDirect

journal homepage: www.elsevier.com/locate/he

Electrochemical and thermal properties of $SmBa_{0.5}Sr_{0.5}Co_2O_{5+\delta}$ cathode impregnated with $Ce_{0.8}Sm_{0.2}O_{1.9}$ nanoparticles for intermediate-temperature solid oxide fuel cells

Adi Subardi [a,b], Yen-Pei Fu [a,*]

[a] Department of Materials Science & Engineering, National Dong Hwa University, Shou-Feng, Hualien 97401, Taiwan

[b] Department of Mechanical Engineering, STTNAS, Yogyakarta 55281, Indonesia

ARTICLE INFO

Article history:
Received 24 April 2017
Received in revised form
21 July 2017
Accepted 7 August 2017
Available online 25 August 2017

Keywords:
Solid oxide fuel cells
Thermal properties
Oxygen vacancy concentration
Impregnation technique
Electrochemical performance

ABSTRACT

$SmBa_{0.5}Sr_{0.5}Co_2O_{5+\delta}$ (SBSC55) impregnated with nano-sized $Ce_{0.8}Sm_{0.2}O_{1.9}$ (SDC) powder has been investigated as a candidate cathode for intermediate-temperature solid oxide fuel cells (IT-SOFCs). The cathode chemical compatibility with electrolyte, thermal expansion behavior, and electrochemical performance are investigated. For compatibility, a good chemical compatibility between SBSC55 and SDC electrolyte is still kept at 1100 °C in air. For thermal dilation curve, it could be divided into two regions, one is the low temperature region (100–265 °C); the other is the high temperature region (265–850 °C). In the low temperature region (100–265 °C), a TEC value is about 17.0×10^{-6} K^{-1} and an increase in slope in the higher temperatures region (265–800 °C), in which a TEC value is around 21.1×10^{-6} K^{-1}. There is an inflection region ranged from 225 to 330 °C in the curve of $d(\delta L/L)/dT$ vs. temperature. The peak inflection point located about 265 °C is associated to the initial temperature for the loss of lattice oxygen and the formation of oxygen vacancies. For electrochemical properties, the polarization resistances (R_p) significantly reduced from 4.17 Ω cm^2 of pure SBSC55 to 1.28 Ω cm^2 of 0.65 mg cm^{-2} of SDC-impregnated SBSC55 at 600 °C. The single cell performance of SBSC55|SDC|Ni-SDC loaded with 0.65 mg cm^{-2} SDC exhibited the optimum power density of 823 mW cm^{-2} at operating temperature of 800 °C. Based on above-mentioned properties, SBSC55 impregnated with an appropriate SDC is potential cathode for IT-SOFCs.

Introduction

Solid-oxide fuel cells (SOFCs) have the prospective for being one of the cleanest and quite a few effective energy for direct transformation of chemical fuels to electricity [1]. The high operating temperature limit the application of SOFCs such as using expensive materials to endure high temperature, while lower operating temperature leads to sluggish oxygen reduction kinetics and high over-potential at the cathode [2,3]. A lower operating temperature can reduce problems with

* Corresponding author.
E-mail address: ypfu@gms.ndhu.edu.tw (Y.-P. Fu).
http://dx.doi.org/10.1016/j.ijhydene.2017.08.010
0360-3199/

sealing and thermal degradation, and allow the use of low-cost metal interconnection materials, and suppress reactions between the cell components, thus lowering the cost of SOFCs. However, the electrochemical activity of the cathode dramatically decreases with decreasing temperature. Generally, the cathode becomes the confining factor in identifying the overall cell performance. Therefore, the exploitation of new electrodes with higher electrocatalytic activities is critical for IT-SOFCs [4,5]. The high performance cathodes with regard to IT-SOFCs mainly based on perovskite structure and its derivative structures. The cobaltites with prominent electrochemical properties have been investigated for IT-SOFC cathode applications [6,7]. They are notable for their superb mixed-ionic-and-electronic conductor (MIEC) performance in the intermediate temperature range. Recently, there have been some reports concerning the impressive oxygen reduction reaction (ORR) for oxygen-deficient layered perovskites. They are suitable for application as cathodes in IT-SOFCs, which require faster oxygen diffusion rates as well as higher surface exchange kinetics at intermediate temperatures range [8,9].

A-site ordered perovskites, $LnBaCo_2O_{5+\delta}$, oxygen can easily migrate through the LnO plane, which was observed via neutron diffraction technique and molecular dynamics simulations [10,11]. In order to improve the oxygen mobility in the LnO plane, many researchers tried to dope different lanthanides and alkali-earth metals into the A-site of oxygen-deficient layered perovskites such as $NdBa_{1-x}Sr_xCo_2O_{5+\delta}$ [12], $GdBa_{0.5}Sr_{0.5}Co_{2-x}Fe_xO_{5+\delta}$ [13,14], $PrBa_{0.5}Sr_{0.5}Co_{2-x}Fe_xO_{5+\delta}$ [15], $Pr_{0.6}Sr_{0.4}Co_2O_{5+\delta}$ [16], $SmBa_{0.5}Sr_{0.5}Co_2O_{5+\delta}$ [17–19]. Mckinlay et al. reported that the substitution of Sr for Ba resulted in a significant increase of conductivity in $YBaCo_2O_{5+\delta}$. The conductivity value of $YBa_{0.5}Sr_{0.5}Co_2O_{5+\delta}$ is much higher than $YBaCo_2O_{5+\delta}$, presumably due to the smaller lattice volume for Sr-substituted specimen [20]. Kim et al. proposed that substitution of Sr for Ba in $GdBaCo_2O_{5+\delta}$ improved chemical stability between the cathode and electrolyte, and expedited oxygen transport [21]. Meng et al. reported that Sr doping in $YBaCo_2O_{5+\delta}$ enhance the electrical conductivity possibly due to the greater amount of electronic holes and mobile interstitial oxygen [22]. Based on the above-mentioned reports, it concludes that the substitution of Sr^{2+} for Ba^{2+} site results in higher electrical conductivity as well as better electrochemical performance of layered perovskites.

In this study, the layered perovskite, $SmBa_{0.5}Sr_{0.5}Co_2O_{5+\delta}$ (SBSC55), is chosen as a cathode material. Although characterization of SBSC55 such as crystal structure, weight loss in air, thermal expansion behavior, microstructure, and electrochemical properties has been investigated, this work was to build on these initial studies and further investigate the thermal expansion behavior via the first derivative δL/L vs. temperature, oxygen vacancy concentration variation, and using impregnation technique to enhance cathode performance.

Experimental

Cathode and electrolyte materials preparation

Stoichiometric amounts of Sm_2O_3 (99%, Wako Pure Chemical Industries, Ltd.), $SrCO_3$ (98%, Shimakyu chemical Co., Ltd), $BaCO_3$ (98.8%, Showa Chemical Industries, Ltd.) and CoO (99,9%, Choneye Pure Chemical Co., Ltd.) powders were used as starting materials. The $SmBa_{0.5}Sr_{0.5}Co_2O_{5+\delta}$ (SBSC55) cathode powders were prepared via the solid-state reaction. The ball-milled mixtures was dried and ground into a powder with mortar and pestle, and then calcined in air at 1100 °C for 4 h [23]. The $Ce_{0.8}Sm_{0.2}O_{1.9}$ (SDC) powder was synthesized by co-precipitation using $Ce(NO_3)_3{\cdot}6H_2O$ (99%, Wako Pure Chemical Industries, Ltd.) and $Sm(NO_3)_3{\cdot}6H_2O$ (99%, Wako Pure Chemical Industries, Ltd.) as the starting materials. These starting materials with stoichiometric ratio were dissolved in distilled water and then added to a solution of ammonia. The pH value of the solution was adjusted to 9.5–10. Then, the coprecipitation powder was calcined in air to 600 °C for 2 h. The detailed procedure regarding the preparation of SDC can refer to reference [24].

The procedure of impregnation technique is based on our group previous published paper as shown in reference [25,26]. Aqueous nitrate solution of $Ce_{0.8}Sm_{0.2}(NO_3)_x$ precursors with different concentrations (0.1, 0.3, 0.5 M) were prepared by dissolving proper amount of $Ce(NO_3)_3{\cdot}6H_2O$ and $Sm(NO_3)_3{\cdot}6H_2O$ in DI water. 3 μL of $Ce_{0.8}Sm_{0.2}(NO_3)_x$ nitration solution were loaded into each side of the porous SBSC55 cathode using a micro-liter syringe in order to control the amount of loading. Finally, the impregnated cell was fired at 900 °C for 2 h to obtain the desired SDC nanoparticles within the SBSC55 skeleton. The loading of SDC can be raised by using higher $Ce_{0.8}Sm_{0.2}(NO_3)_x$ nitrate solution. For example, one impregnated with 3 μL of 0.1 M $Ce_{0.8}Sm_{0.2}(NO_3)_x$ nitrate solution will give an SDC loading of 0.13 mg cm^{-2} in SBSC55 with effective area of 0.385 cm^2.

Material characterization

The structure of the SBSC55 cathode and the chemical compatibility between SBSC55 cathode and SDC electrolyte were characterized by X-ray powder diffractometer (XRD; Rigaku D/MAX-2500V), with a scanning rate of 2°/min and scanning range of 20–80°, using a Cu K_α (1.5418 Å) radiation source. The microstructures of the SBSC55 cathode was observed by scanning electron microscope (SEM; Hitachi 3500H). The thermogravimetric properties of calcined powder specimen were performed using a thermogravimetric analyzer (TGA; SII TG/DTA 6300) in static air from room temperature to 800 °C using a constant heating rate of 10 °C/min, and the TGA measurements were performed in air and N_2. The thermal expansion coefficient (TEC) of the SBSC55 sintered at 1100 °C for 4 h was measured using a thermomechanical analyzer (TMA; Hitachi TMA7300) with a constant heating rate of 10C/min in the temperature range of 25–800 °C in a static air.

Symmetrical cell fabrication and measurement

The symmetrical cells of SBSC55 and SDC-loaded SBSC55 were fabricated by screen-printing technique. The SBSC55-based cathode was pasted on both sides of SDC electrolyte discs in circles of 13 mm diameter and 1 mm thick. After the cathode was painted on the SDC electrolyte, it was sintered at 1000 °C for 4 h in air. The cathode was used as the working electrode

(WE) with surface area of 0.385 cm^2. The Ag reference electrode (RE) was placed away from the WE by about 0.3–0.4 cm. The SBSC55-based cathode counter electrode (CE) was placed on the other side of the SDC disk. The symmetrical testing cell experiments were carried out under $p(O_2)$ = 0.21 atm in temperatures ranging from 600 to 800 °C at intervals of 50 °C in a furnace. The AC impedance measurement was performed using the VoltaLab PGZ301 potentiostat with frequency applied range from 100 kHz to 0.1 Hz with 10 mV AC signal amplitude. Under the cathodic polarized condition, the EIS was conducted as a function of the applied cathodic voltage. The EIS fitting analysis was performed with the Z-view software.

Single cell fabrication and measurement

Button cells were measured with humidified hydrogen (3 vol% H_2O) as the fuel and air as the oxidant to evaluate the performance of the fabricated anode-supported SOFCs. The current-voltage characteristics of the single cells were collected using a digital source meter (Keithley 2420) at intervals of 100 °C over a temperature range of 500–800 °C.

Result and discussion

Material characterization of SBSC55

To study the chemical compatibility of cathode, the evaluation of chemical interaction between the SBSC55 cathode and SDC electrolyte was conducted. Fig. 1 shows the XRD patterns of the powder mixture of 70 wt% SBSC55 + 30 wt% SDC calcined at various temperatures. The solid-state reaction between SBSC55 and SDC phases is very important to evaluate their chemical stability at high temperature. SBSC55 is a double-perovskite structure with space group of *P4/mmm*, lattice parameter, a = 3.88 Å, b = 3.88 Å, c = 7.58 Å, and v = 114.30 $Å^3$, while SDC is a cubic fluorite-type structure. The results reveal that no obvious interface reaction appeared for 70 wt% SBSC55 mixed with 30 wt% SDC composite when heated up to 1100 °C for 4 h.

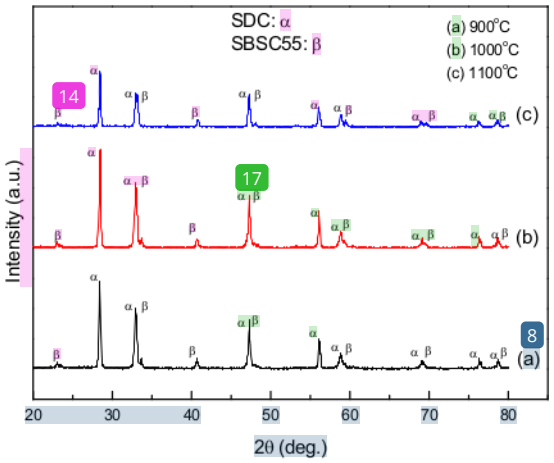

Fig. 1 – X-ray powder diffraction patterns for the powder mixture of 70 wt% SBSC55 + 30 wt% SDC heat-treatment at (a) 900 °C, (b) 1000 °C and (c) 1100 °C for 4 h.

Oxygen vacancy concentration variation and thermal expansion behavior

In order to determine the oxygen vacancy concentration variation of calcined SBSC55, the weight loss of specimen in air and N_2 atmosphere were conducted. The difference between ideal oxygen stoichiometry (δ) and oxygen vacancy concentration variation (ΔC_v) of the calcined powder at different temperature could be defined as follows [27].

$$\Delta C_v \approx \left(\frac{\rho}{M}\right)\left(\Delta W_{N_2}\% - \Delta W_{air}\%\right) \quad (1)$$

in which, ρ and *M* are the theoretical density (g/cm^3) and molar weight (g/mol) of the oxygen atom for the specimen, respectively; ΔW_{air}%, and ΔW_{N2}% are the percentage of weight difference in air and N_2 atmosphere, respectively. The oxygen vacancy concentration variation of the calcined SBSC55 powder in air and N_2 atmosphere is shown in Fig. 2(a), and it is assumed that the ideal oxygen stoichiometry (δ) is same at room temperature in air and N_2 atmosphere. The oxygen vacancy concentration variation is increased with temperature,

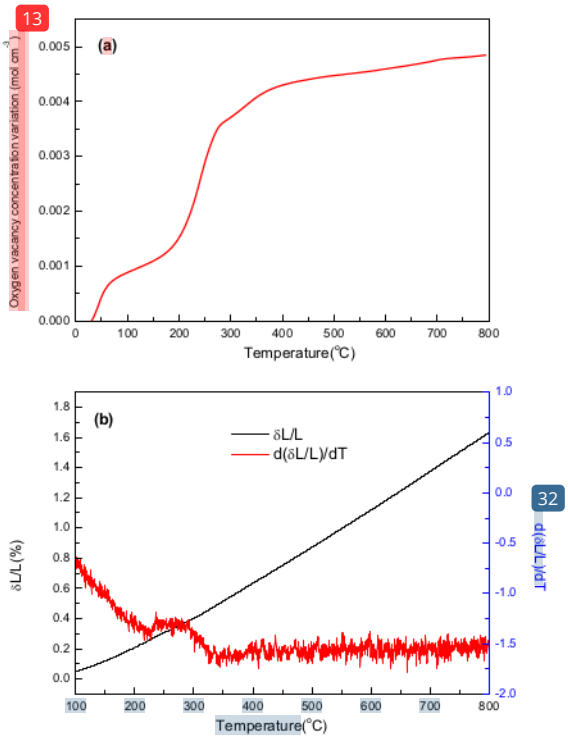

Fig. 2 – (a) Oxygen vacancy concentration differences for calcined SBSC55 powder; (b) Thermal expansion curves for δL/L and first derivative δL/L as a function of temperature for sintered SBSC55 bulk.

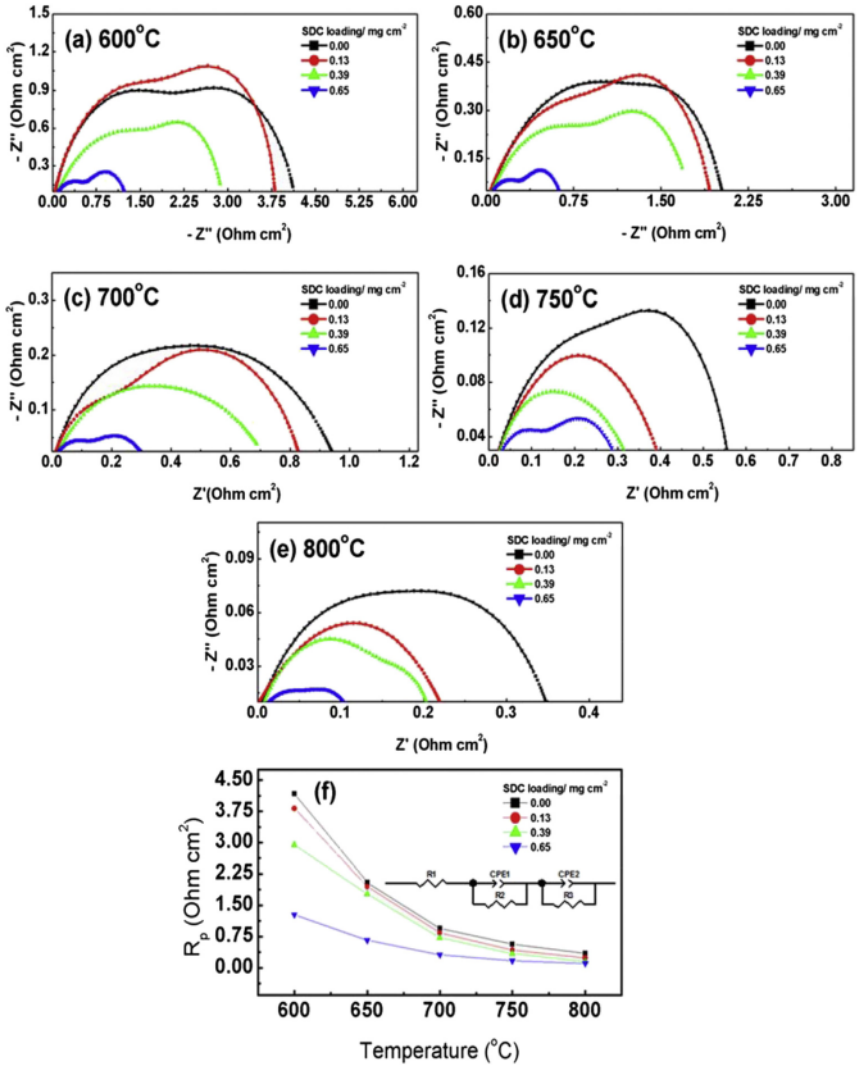

Fig. 3 – Typical impedance spectra of SDC-impregnated SBSC55 cathode as a function of SDC-loaded amount at (a) 600, (b) 650, (c) 700, (d) 750, (e) 800 °C and (f) total cathode polarization resistance (R_p) over the temperature range of 600–800 °C.

and the oxygen vacancy concentration variation enhances dramatically in temperature range of 180–280 °C. It is speculated that great amount of Co^{4+} ions are reduced to Co^{3+} with large amount of oxygen loss as same as thermal expansion behavior that we will discuss later.

The thermal expansion coefficient (TEC) is a crucial property for cathode materials as it governs the performance of a single cell. A bulk thermal expansion curve for SBSC55 cathode was measured from room temperature to 800 °C using a thermomechanical analyzer as shown in Fig. 2(b). The SBSC55 specimens seemingly show a linear expansion; however, in the first derivative δL/L plot, the thermal expansion curve could be divided into two regions, one is the low temperature region (100–265 °C); the other is the high temperature region (265–800 °C). The TEC calculated from 100 to 800 °C for SBSC55 is 19.8 × 10^{-6} K^{-1}. However, in the low temperature region (100–265 °C), a TEC value is about 17.0 × 10^{-6} K^{-1} and an increase in slope in the higher temperatures region (265–800 °C), in which a TEC value is around 21.1 × 10^{-6} K^{-1}. As seen in the curve of $d(\delta L/L)/dT$ vs. temperature, there is an inflection region ranged from 225 to 330 °C. The peak inflection point located about 265 °C is associated to the initial temperature for the loss of lattice oxygen and the formation of oxygen vacancies [28]. Meanwhile, the reduction in Co valence has to take place to maintain the electrical neutrality. As the temperature is elevated above 265 °C, a part of Co^{4+} ions are reduced to Co^{3+} with a loss of oxygen; and Co^{3+} ions transit from low-spin ($t_{2g}^6e_g^0$) to high-spin ($t_{2g}^4e_g^2$) states [29,30]. The relationship based on the defect reaction using the Kroger-Vink notation is described as follows.

$$2Co_{Co}^{\cdot} + O_O^{\times} \leftrightarrow 2Co_{Co}^{\times} + V_{\ddot{o}} + \frac{1}{2}O_2 \quad (Co^{4+} \rightarrow Co^{3+}) \qquad (2)$$

The Co-valence transfers are highly related to ionic radius. The ionic radium of Co^{4+} and Co^{3+} with the coordination number of 6 and high spin are 0.53 and 0.61 nm, respectively [31]. The reduction of Co ions leads a decrease in the B–O bond based on Pauling's second rule, resulting in an increase in the size of BO_6 octahedra; therefore, the lattice expansion is enhanced [32,33]. Generally, cobalt-based perovskite with a larger TECs can be due to the increase of the ionic radius of Co during the thermal expansion measurement [34].

Electrochemical properties

In order to evaluate the effect of SDC-impregnated SBSC55 cathode on electrochemical properties, various SDC amount loaded on SBSC55|SDC half-cells were tested. The EIS and R_p were recorded as a function of SDC loading amount under stationary air as the oxidant ranged from 600 to 800 °C as shown in Fig. 3(a)–(e) present some typical impedance spectra of SBSC55 cathode with and without SDC impregnation measured in symmetrical cells using AC impedance spectroscopy under open circuit conditions at various temperatures in air. After SDC nanoparticles impregnate on SBSC55 porous skeleton, there was a significant reduction in the impedance for oxygen reduction reaction for SBSC55 electrode, indicating the enhancement of the electrochemical activity. The polarization resistances (R_p) of SBSC55 cathode reduced from 4.17 Ω cm^2 of 600 °C to 0.35 Ω cm^2 of 800 °C. When SDC electrolyte loaded on pure SBSC55 cathode, the R_p values are significantly reduced, indicating that both electrochemical processes (i.e., the electrochemical reactions at the electrode–electrolyte interface and the adsorption–desorption of oxygen diffusion at the gas-cathode surface interface) were simultaneously improved by active SDC nano-sized particles. When 0.13 mg cm^{-2} SDC loaded onto the porous SBSC55, R_p values gradually reduces from 3.82 Ω cm^2 of 600 °C to 0.24 Ω cm^2 of 800 °C. When SDC-loaded amount was increased to 0.65 mg cm^{-2}, the R_p values are further reduced to 1.28, 0.32, and 0.11 Ω cm^2 at 600 °C, 700 °C, and 800 °C, respectively. The R_p values of the symmetrical cells with various types of SBSC55 cathode are summarized in Fig. 3(f). The R_p values exhibited visible distinctions and followed the sequence of pure SBSC55 > 0.13 mg cm^{-2} SDC-impregnated SBSC55 > 0.39 mg cm^{-2} SDC-impregnated SBSC55 > 0.65 mg cm^{-2} SDC- impregnated SBSC55 within the temperature range of 600–800 °C. The decrease in R_p was mainly attributed to the creation of extra SDC/SBSC55 phase boundaries. The newly formed nano-sized SDC particles upon the highly porous SBSC55 surface allowed gas-phase molecules to easily diffuse to the SDC/SBSC55 boundaries, which considerably increased the number of electrochemical sites for the ORR. The ORR sites were at the real SBSC55 cathode surface area simultaneously exposed to electrolyte and air as well as at these newly formed SDC nanoparticles deposited on SBSC55 porous skeleton. Table 1 lists the detailed cathodic polarization resistances of SBSC55 cathode.

The exchange current density (i_o) value is an important information to evaluate the intrinsic oxygen reduction rate and the electrochemical properties of cathode. In the present work, the i_o values were identified using electrochemical impedance spectrometry (EIS), i_o values were determined from the R_p of the Nyquist plot as depicted in Fig. 4. The detailed information regarding the EIS technique could refer to our group published paper [23]. Generally, the i_0 values is rising with temperature. The i_o values were increased from 4.5 mA cm^{-2} of 600 °C to 64.1 mA cm^{-2} of 800 °C. As nano-sized SDC powder loaded into SBSC55, the i_o values are significantly enhanced. For example, SBSC55 cathode loaded with 0.65 mg cm^{-2} SDC, the i_o values were enhanced from 14.8 mA cm^{-2} of 600 °C to 165.7 mA cm^{-2} of 800 °C as listed in Table 2. The overall activation energy (E_a) for the ORR was identified from the slope of the Arrhenius plots as shown in

Table 1 – Polarization resistance of SBSC55 cathode impregnated with different SDC-loaded amount.

SDC-loaded amount (mg cm^{-2})	R_p (Ω cm^2)				
	600 °C	650 °C	700 °C	750 °C	800 °C
0.00	4.17	2.05	0.95	0.57	0.36
0.13	3.82	1.95	0.84	0.43	0.24
0.39	2.95	1.77	0.73	0.35	0.15
0.65	1.28	0.66	0.32	0.18	0.12

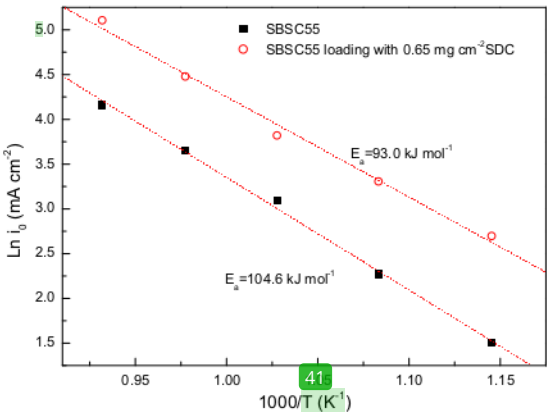

Fig. 4 – Arrhenius plots of ORR for SBSC55 and 0.65 mg cm^{-2} SDC-impregnated SBSC55, i_o was obtained using EIS technique.

Table 2 – Exchange current density, i_o of ORR for the SBSC55 and 0.65 mg cm^{-2} SDC-impregnated SBSC55 cathode using EIS technique over the temperature range of 600–800 °C.

T(°C)	i_o (mA cm^2)	
	SBSC55	With 0.65 mg cm^{-2} SDC loaded
600	4.5	14.8
650	9.7	27.4
700	22.0	45.6
750	38.5	88.2
800	64.1	165.7

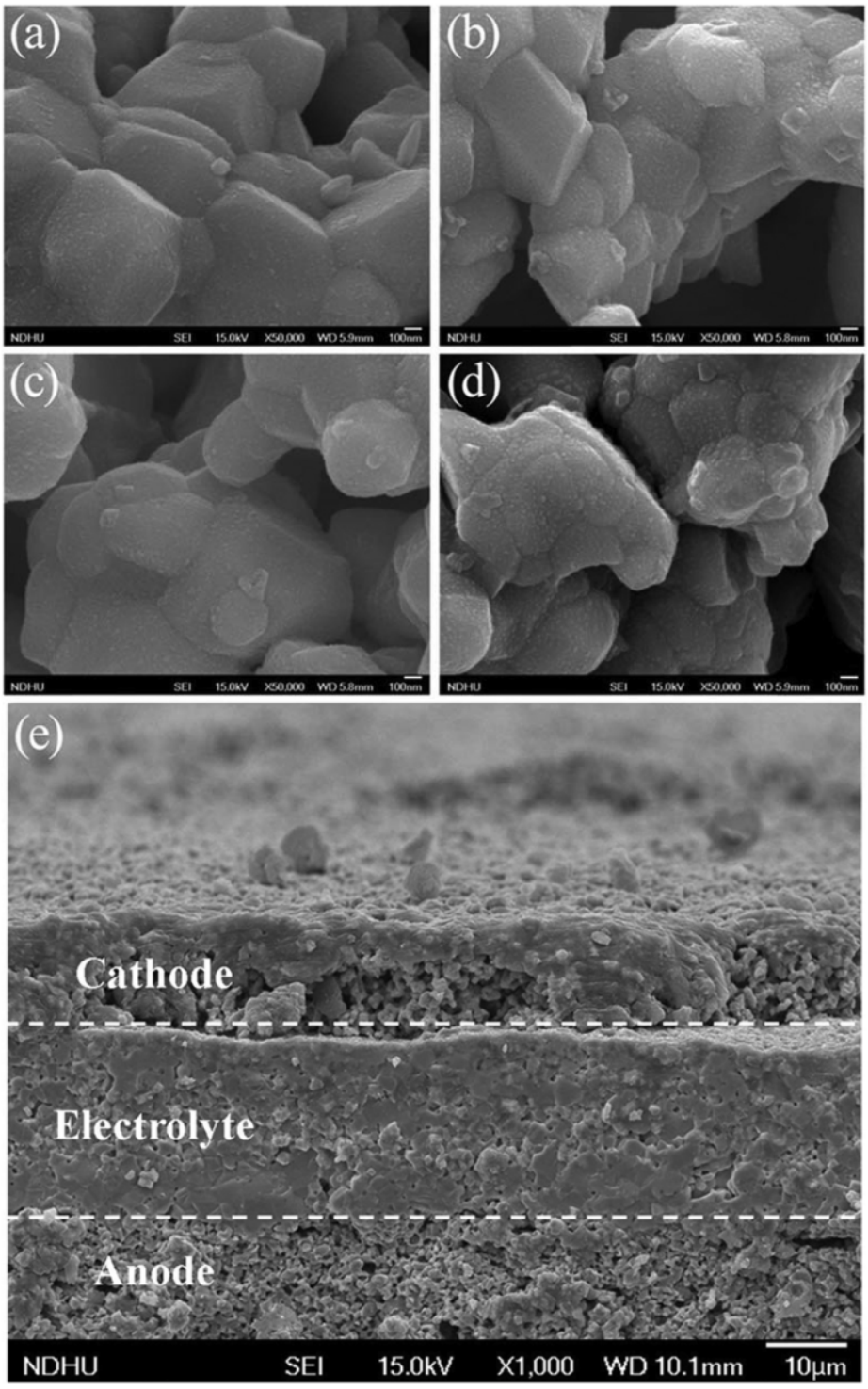

Fig. 5 – SEM micrographs for (a) pure SBSC55, (b) 0.13 mg cm^{-2} SDC-impregnated SBSC55, (c) 0.39 mg cm^{-2} SDC-impregnated SBSC55, (d) 0.65 mg cm^{-2} SDC-impregnated SBSC55 and (e) cross-sectional view of the single cell of (d).

Fig. 4. The E_a values were 104.6 and 93.0 kJ mol^{-1} for SBSC55 and 0.65 mg cm^{-2} SDC-loading SBSC55, respectively. The linearity of the Arrhenius plots implying that SBSC55-based cathode are stable as a function of temperature. The activation value is relatively similar to our previous report as cited in reference [23].

SEM images

To improve the cathode performance, the active ionic-conductive SDC nano-sized particles were deposited on a porous SBSC55 backbones via impregnation technique. The microstructures of the SBSC55 impregnated with various SDC loading and the cross section were observed by FESEM. The SBSC55 cathode without impregnated SDC electrolyte is shown in Fig. 5(a). When using impregnation technique, SDC nanoparticles deposited onto backbones of SBSC55 resulting in the increase in the ORR sites and enhancement of cathode electrochemical properties. The SDC nano-particles are uniformly coated on the skeleton of the SBSC55 pores, as seen in Fig. 5(b)–(d). The uniform coating and homogeneous distribution on the porous SBSC55 backbones results in good interconnection and enhanced electrochemical properties. When 0.13 mg cm^{-2} SDC impregnated with, it can be seen that the particle size of SDC was about 10–20 coating on SBSC55. When SDC-loading amount reached to 0.65 mg cm^{-2}, SDC nanoparticles gradually grew in the range of 20–35 nm. Fig. 5(e) shows the cross-sectional view of the 0.65 mg cm^{-2} SDC-impregnated SBSC55|SDC|Ni-SDC with a 15 μm of cathode and 24 μm of electrolyte. The adhesion between the cathode, electrolyte, and anode reveals well, and the electrolyte membrane is well sintered and quite dense. The cathode and the anode are both highly porous providing gas-flowing path.

Performance of the assembling single-cells

Fig. 6 plots the single cell performances for anode-supported Ni-SDC|SDC|SBSC55 SOFC using humidified hydrogen (3 vol% H_2O) as the fuel and air as the oxidant. In general, the cell voltage was reduced with the increasing temperature; however, current density and the maximum power densities were increased with the increasing temperature due to the thermally activated process of kinetics [35]. The current-voltage curves and the corresponding power densities for pure SBSC55 assembling single cell at various operating temperatures are shown in Fig. 6(a). The peak power densities are 370, 485 and 470 mW cm^{-2} at 600 °C, 700 °C, and 800 °C, respectively. When 0.13 mg cm^{-2} of SDC loaded into the SBSC55 cathode (Fig. 6(b)), the peak power densities of single cell were increased to 538, 620 and 665 mW cm^{-2} at 600 °C, 700 °C, and 800 °C, respectively. As the SDC-loaded amount was increased to 0.39 mg cm^{-2} (Fig. 6(c)), the peak power densities were further increased to 696, 755 and 815 mW cm^{-2} at 600 °C, 700 °C, and 800 °C, respectively. When the SDC-loaded amount reached to 0.65 mg cm^{-2} (Fig. 6(d)), the peak power densities achieved 740, 815, and 823 mW cm^{-2} at 600 °C, 700 °C, and 800 °C, respectively. Obviously, the SBSC55 cathode loaded with 0.65 mg cm^{-2} SDC operating at 800 °C reached the maximum peak power density of 823 mW cm^{-2}. Regarding the power density values, some layered perovskite cathodes had been reported such as, the power density at 650 °C for $NdBa_{0.5}Sr_{0.5}Co_{1.5}Fe_{0.5}O_{5+\delta}$ is 650 mW cm^{-2} [36], at 700 °C for $Nd_{0.96}BaCo_2O_{6-\delta}$ is 600 mW cm^{-2} [37], at 800 °C for $SmBa_{0.75}Ca_{0.25}CoFeO_{5+\delta}$ is 366 mW cm^{-2} [38]. This result implies that the impregnation of the electrolyte with nano-sized into the porous cathode backbones indeed improved the electrochemical performance of the single cell.

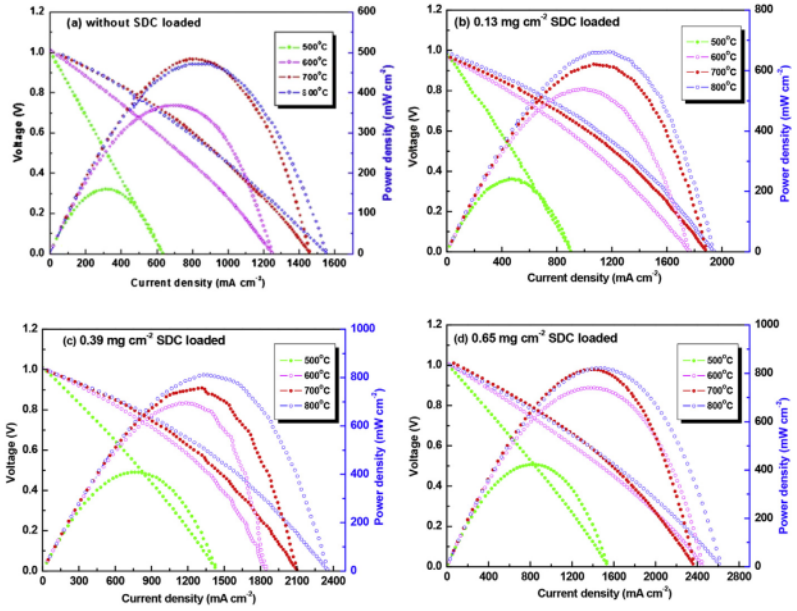

Fig. 6 – I-V curve for a single cell at various temperatures between 500 and 800 °C: (a) pure SBSC55, (b) 0.13 mg cm^{-2} SDC-impregnated SBSC55, (c) 0.39 mg cm^{-2} SDC- impregnated SBSC55 and (d) 0.65 mg cm^{-2} SDC-impregnated SBSC55.

Conclusions

This study mainly investigated chemical compatibility, thermal properties, oxygen vacancy concentration variation, electrochemical properties, and single-cell performance for SBSC55. The concentration of Co^{4+} ion in SBSC55 decreased significantly above 265 °C due to loss of lattice oxygen ($Co^{4+} \rightarrow Co^{3+}$) and creation of $V_{\ddot{o}}$ simultaneously. The single cell for 0.65 mg cm^{-2} SDC loaded onto SBSC55 showed the optimum performance of 823 mW cm^{-2} at operating temperature of 800 °C, which is associated with higher electrical conductivity, fast oxygen transport at the surface, and high catalytic activity for the oxygen reduction reaction. Therefore, $SmBa_{0.5}Sr_{0.5}Co_2O_{5+\delta}$ impregnated with SDC nanoparticles is desirable candidate cathode materials in IT-SOFCs in accordance with electrochemical performance.

Acknowledgements

The authors are grateful for the financial support of this research by Ministry of Science and Technology of Taiwan under contract number: MOST 105-2119-M-259-003 and MOST 105-2119-M-259-002.

REFERENCES

[1] Ding D, Li X, Lai SY, Gerdes K, Liu M. Enhancing SOFC performance by surface modification through infiltration. Energy Environ Sci 2014;7:552–75.
[2] Ding L, Wang L, Ding D, Zhang S, Ding X, Yuan G. Promotion on electrochemical performance of a cation deficient $SrCo_{0.7}Nb_{0.1}Fe_{0.2}O_{3-\delta}$ perovskite cathode for intermediate temperature solid oxide fuel cells. J Power Sources 2017;354:26–33.
[3] Das D, Basu RN. Improved polarization behaviour of nanostructured $La_{0.65}Sr_{0.3}MnO_3$ cathode with engineered morphology. Int J Hydrogen Energy 2017;42:15347–58.
[4] Olsson E, Aparicio-Angles X, de Leeuw NH. A computational study of the electronic properties, ionic conduction, and thermal expansion of $Sm_{(1-x)}A_{(x)}CoO_{(3)}$ and $Sm_{(1-x)}A_{(x)}CoO_{(3-x/2)}$ ($A = Ba^{2+}$, Ca^{2+}, Sr^{2+}, and x=0.25, 0.5) as intermediate temperature SOFC cathodes. Phys Chem Chem Phys 2017;19:13960–9.
[5] Giuliano A, Carpanese MP, Panizza M, Cerisola G, Clematis D, Barbucci A. Characterisation of $La_{0.6}Sr_{0.4}Co_{0.2}Fe_{0.8}O_{3-\delta}$-$Ba_{0.5}Sr_{0.5}Co_{0.8}Fe_{0.2}O_{3-\delta}$ composite as cathode for solid oxide fuel cells. Electrochim Acta 2017;240:258–66.
[6] Jiang XN, Wang J, Jia GQ, Qie ZJ, Shi YC, Idrees A, et al. Characterization of $PrBa_{0.92}CoCuO_{6-\delta}$ as a potential cathode material of intermediate-temperature solid oxide fuel cell. Int J Hydrogen Energy 2017;42:6281–9.
[7] Gomez AEM, Lamas DG, Leyva AG, Sacanell J. Nanostructured $LnBaCo_2O_{6-\delta}$ (Ln = Sm, Gd) with layered structure for intermediate temperature solid oxide fuel cell cathodes. AIP Adv 2017;7, 045214.
[8] Tarancón A, Burriel M, Santiso J, Skinner SJ, Kilner JA. Advances in layered oxide cathodes for intermediate temperature solid oxide fuel cells. J Mater Chem 2010;20:3799–813.
[9] Lee Y, Kim DY, Choi GM. $GdBaCo_2O_{5+x}$ cathode for anode-supported ceria SOFCs. Solid State Ionics 2011;192:527–30.
[10] Frontera C, Caneiro A, Carrillo AE, Oró-Solé J, García-Muñoz JL. Tailoring oxygen content on $PrBaCo_2O_{5+\delta}$ layered cobaltites. Chem Mater 2005;17:5439–45.
[11] Parfitt D, Chroneos A, Tarancón A, Kilner JA. Oxygen ion diffusion in cation ordered/disordered $GdBaCo_2O_{5+\delta}$. J Mater Chem 2011;21:2183–6.
[12] Kim JH, Irvine JTS. Characterization of layered perovskite oxides $NdBa_{1-x}Sr_xCo_2O_{5-\delta}$ (x = 0 and 0.5) as cathode materials for IT-SOFC. Int J Hydrogen Energy 2012;37:5920–9.
[13] Kuroda C, Zheng K, Swierczek K. Characterization of novel $GdBa_{0.5}Sr_{0.5}Co_{2-x}Fe_xO_{5+\delta}$ perovskites for application in IT-SOFC cells. Int J Hydrogen Energy 2013;38:1027–38.
[14] Kim J, Jun A, Shin J, Kim G. Effect of Fe doping on layered $GdBa_{0.5}Sr_{0.5}Co_2O_{5+\delta}$ perovskite cathodes for intermediate temperature solid oxide fuel cells. J Am Ceram Soc 2014;97:651–6.
[15] Jiang L, Wei T, Zeng R, Zhang WX, Huang YH. Thermal and electrochemical properties of $PrBa_{0.5}Sr_{0.5}Co_{2-x}Fe_xO_{5+\delta}$ (x = 0.5, 1.0, 1.5) cathode materials for solid-oxide fuel cells. J Power Sources 2013;232:279–85.
[16] Xue J, Shen Y, He T. Performance of double-perovskite $YBa_{0.5}Sr_{0.5}Co_2O_{5-\delta}$ as cathode material for intermediate-temperature solid oxide fuel cells. Int J Hydrogen Energy 2011;36:6894–8.
[17] Kim JH, Cassidy M, Irvine JTS, Bae J. Advanced electrochemical properties of $LnBa_{0.5}Sr_{0.5}Co_2O_{5+\delta}$ (Ln= Pr, Sm, and Gd) as cathode materials for IT-SOFC. J Electrochem Soc 2009;156:B682–9.
[18] Kim JH, Cassidy M, Irvine JTS, Bae J. Electrochemical investigation of composite cathodes with $SmBa_{0.5}Sr_{0.5}Co_2O_{5+\delta}$ cathodes for intermediate temperature-operating solid oxide fuel cell. Chem Mater 2010;22:883–92.
[19] Jun A, Kim J, Shin J, Kim G. Optimization of Sr content in layered $SmBa_{1-x}Sr_xCo_2O_{5+\delta}$ perovskite cathodes for intermediate-temperature solid oxide fuel cells. Int J Hydrogen Energy 2012;37:18381–8.
[20] McKinlay A, Connor P, Irvine JTS, Zhou WZ. Structural chemistry and conductivity of solid solution $YBa_{1-x}Sr_xCo_2O_{5+\delta}$. J Phys Chem C 2007;111:19120–5.
[21] Kim JH, Prado F, Manthiram A. Characterization of $GdBa_{1-x}Sr_xCo_2O_{5+\delta}$ ($0 \leq x \leq 1.0$) double perovskites as cathodes for solid oxide fuel cells. J Electrochem Soc 2008;155:B1023–8.
[22] Meng F, Xia T, Wang J, Shi Z, Lian J, Zhao H, et al. Evaluation of layered perovskites $YBa_{1-}xSrxCo_2O_{5+\delta}$ as cathodes for intermediate-temperature solid oxide fuel cells. Int J Hydrogen Energy 2014;39:4531–43.
[23] Subardi A, Cheng MH, Fu YP. Chemical bulk diffusion and electrochemical properties of $SmBa_{0.6}Sr_{0.4}Co_2O_{5+\delta}$ cathode for intermediate solid oxide fuel cells. Int J Hydrogen Energy 2014;39:20783–90.
[24] Fu YP, Wen SB, Lu CH. Preparation and characterization of samaria-doped ceria electrolyte materials for solid oxide fuel cells. J Am Ceram Soc 2008;91:127–31.
[25] Kuhn M, Kim JJ, Bishop SR, Tuller HL. Oxygen nonstoichiometry and defect chemistry of perovskite-structured $Ba_xSr_{1-x}Ti_{1-y}Fe_yO_{3-y/2+\delta}$ solid solutions. Chem Mater 2013;25:2970–5.
[26] Fu YP, Hsieh MY. Chemical bulk diffusion coefficient of a $La_{0.5}Sr_{0.5}CoO_{3-\delta}$ cathode for intermediate-temperature solid oxide fuel cells. J Am Ceram Soc 2014;97:3230–7.
[27] Lia S, Jin W, Xu N, Shi J. Mechanical strength, and oxygen and electronic transport properties of $SrCo_{0.4}Fe_{0.6}O_{3-\delta}$-YSZ membranes. J Membr Sci 2001;186:195–204.

[28] Teraoka Y, Yoshimatsu M, Yamazoe N, Seiyama T. Oxygen-sorptive properties and defect structure of perovskite-type oxides. Chem Lett 1984:893–6.
[29] Huang K, Lee HY, Goodenough JB. Sr- and Ni-doped $LaCoO_3$ and $LaFeO_3$ perovskites new cathode materials for solid-oxide fuel cells. J Electrochem Soc 1998; 145:3220–7.
[30] Senaris-Rodriguez MA, Goodenough JB. $LaCoO_3$ revisited. J Solid State Chem 1995;116:224–31.
[31] Shannon RD. Revised effective ionic radii and systematic studies of interatomic distances in halides and chalcogenides. Acta Crystallogr A 1976;32:751–67.
[32] Kostogloudis GCh, Fertis P, Ftikos Ch. The perovskite oxide system $Pr_{1-x}Sr_xCo_{1-y}Mn_yO_{3-\delta}$: crystal structure and thermal expansion. J Eur Ceram Soc 1998;18:2209–15.
[33] Wei B, Lu Z, Huang X, Miao J, Sha X, Xin X, et al. J Eur Ceram Soc 2006;26:2827–32.
[34] Mori M, Sammes NM. Sintering and thermal expansion characterization of Al-doped and Co-doped lanthanum strontium chromites synthesized by the Pechini method. Solid State Ionics 2002;146:301–12.
[35] Vashook VV, Tolochko SP, Yushkevich II, Makhnach LV, Kononyuk IF, Altenburg H, et al. Oxygen nonstoichiometry and electrical conductivity of the solid solutions $La_{2-x}Sr_xNiO_y$ ($0 \leq x \leq 0.5$). Solid State Ionics 1998;110:245–53.
[36] Lee TH, Park KY, Kim NI, Song SJ, Hong KH, Ahn D, et al. Robust $NdBa_{0.5}Sr_{0.5}Co_{1.5}Fe_{0.5}O_{5+\delta}$ cathode material and its degradation prevention operating logic for intermediate temperatures solid oxide fuel cells. J Power Sources 2016;331:495–506.
[37] Yi K, Sun L, Li Q, Xia T, Huo L, Zhao H, et al. Effect of Nd-deficiency on electrochemical properties of $NdBaCo_2O_{6-\delta}$ cathode for intermediate-temperature solid oxide fuel cells. Int J Hydrogen Energy 2016;41:10228–38.
[38] Zheng Y, Zhang Y, Yu F, Pan Z, Yang H, Guo L. Ca and Fe co-doped $SmBaCo_2O_{5+\delta}$ layered perovskite as an efficient cathode for intermediate-temperature solid oxide fuel cells. J Alloys Compd 2017;696:964–70.

Electrochemical and thermal properties of SmBa0.5Sr0.5Co2O5þd cathode impregnated with Ce0.8Sm0.2O1.9 nanoparticles for intermediate- temperature solid oxide fuel cells

ORIGINALITY REPORT

16%	11%	12%	3%
SIMILARITY INDEX	INTERNET SOURCES	PUBLICATIONS	STUDENT PAPERS

PRIMARY SOURCES

1	sinta3.ristekdikti.go.id Internet Source	1%
2	www.norecs.com Internet Source	1%
3	uu.diva-portal.org Internet Source	<1%
4	Atul Verma, Sanath Kumar, Yen-Pei Fu. "A ternary-hybrid as efficiently photocatalytic antibiotic degradation and electrochemical pollutant detection", Chemical Engineering Journal, 2021 Publication	<1%
5	pdfs.semanticscholar.org Internet Source	<1%
6	Fu, Y.P.. "Comparison of microwave-induced combustion and solid-state reaction for synthesis of LiMn"2"-"xCr"xO"4 powders and	<1%

their electrochemical properties", Solid State Ionics, 20040115
Publication

7	dr.ntu.edu.sg Internet Source	<1 %
8	rep.ksu.kz Internet Source	<1 %
9	repositories.lib.utexas.edu Internet Source	<1 %
10	www.preprints.org Internet Source	<1 %
11	Baitao Li, Kenji Maruyama, Mohammad Nurunnabi, Kimio Kunimori, Keiichi Tomishige. " Effect of Ni Loading on Catalyst Bed Temperature in Oxidative Steam Reforming of Methane over α-Al O -Supported Ni Catalysts ", Industrial & Engineering Chemistry Research, 2005 Publication	<1 %
12	Submitted to Pennsylvania State System of Higher Education Student Paper	<1 %
13	Shiguang Li, Wanqin Jin, Pei Huang, Nanping Xu, Jun Shi, Y. S. Lin, Michael Z.-C. Hu, E. Andrew Payzant. " Comparison of Oxygen Permeability and Stability of Perovskite Type La A Co Fe O (A = Sr, Ba, Ca) Membranes ",	<1 %

	Industrial & Engineering Chemistry Research, 1999 Publication	
14	mro.massey.ac.nz Internet Source	<1 %
15	Karthik S. Bhat, Harish C. Barshilia, H.S. Nagaraja. "Porous nickel telluride nanostructures as bifunctional electrocatalyst towards hydrogen and oxygen evolution reaction", International Journal of Hydrogen Energy, 2017 Publication	<1 %
16	riunet.upv.es Internet Source	<1 %
17	Submitted to Harper Adams University College Student Paper	<1 %
18	Kilner, John A., and Mónica Burriel. "Materials for Intermediate-Temperature Solid-Oxide Fuel Cells", Annual Review of Materials Research, 2013. Publication	<1 %
19	Lin XIONG, Shaorong WANG, Zhenrong WANG, Tinglian WEN. "Effect of samarium doped ceria nanoparticles impregnation on the performance of anode supported SOFC	<1 %

with (Pr0.7Ca0.3)0.9MnO3−δ cathode", Journal of Rare Earths, 2010
Publication

20	Submitted to Swinburne University of Technology Student Paper	<1 %
21	Submitted to University of Surrey Student Paper	<1 %
22	Zhu, W.. "Ceria coated Ni as anodes for direct utilization of methane in low-temperature solid oxide fuel cells", Journal of Power Sources, 20061006 Publication	<1 %
23	ceramics.hfut.edu.cn Internet Source	<1 %
24	jultika.oulu.fi Internet Source	<1 %
25	pure.uva.nl Internet Source	<1 %
26	Submitted to Imperial College of Science, Technology and Medicine Student Paper	<1 %
27	Jun, Areum, Tak-hyoung Lim, Jeeyoung Shin, and Guntae Kim. "Electrochemical properties of B-site Ni doped layered perovskite	<1 %

cathodes for IT-SOFCs", International Journal of Hydrogen Energy, 2014.
Publication

28	fisica.cab.cnea.gov.ar Internet Source	<1 %
29	www2.mdpi.com Internet Source	<1 %
30	Submitted to Universiti Kebangsaan Malaysia Student Paper	<1 %
31	Xue, J.. "Performance of double-proveskite YBa"0"."5Sr"0"."5Co"2O"5"+"@d as cathode material for intermediate-temperature solid oxide fuel cells", International Journal of Hydrogen Energy, 201105 Publication	<1 %
32	d-nb.info Internet Source	<1 %
33	edepositireland.ie Internet Source	<1 %
34	orbit.dtu.dk Internet Source	<1 %
35	tel.archives-ouvertes.fr Internet Source	<1 %
36	Andreas Løken, Sandrine Ricote, Sebastian Wachowski. "Thermal and Chemical Expansion in Proton Ceramic Electrolytes and	<1 %

Compatible Electrodes", Crystals, 2018
Publication

37	Ma, Q.. "Direct utilization of ammonia in intermediate-temperature solid oxide fuel cells", Electrochemistry Communications, 200611 Publication	<1 %
38	Yang, Z.H.. "Fabrication and characterization of amorphous SiBCN powders", Ceramics International, 200712 Publication	<1 %
39	dspace.uowm.gr Internet Source	<1 %
40	epdf.tips Internet Source	<1 %
41	theses.lib.polyu.edu.hk Internet Source	<1 %
42	"Perovskite and Derivative Compounds as Mixed Ionic-Electronic Conductors", Perovskites and Related Mixed Oxides, 2015. Publication	<1 %
43	Bo Wei, Zhe Lü, Dechang Jia, Tianshi Wei, Xiqiang Huang, Yaohui Zhang, Wenhui Su. " Significantly Enhanced Performance of the GdBaCo O Cathodes with Active Ce Sm O Nanoparticles ", ECS Meeting Abstracts, 2010 Publication	<1 %

44	Chuangang Yao, Jixing Yang, Haixia Zhang, Sigeng Chen, Jian Meng, Kedi Cai. " Characterization of (= 0, 0.1 and 0.2) as cathode for intermediate - temperature solid oxide fuel cells ", International Journal of Energy Research, 2020 Publication	<1 %
45	Heiner Jakob Gores, Hans-Georg Schweiger, Woong-Ki Kim. "Chapter 443 Optimization of Electrolyte Properties by Simplex Exemplified for Conductivity of Lithium Battery Electrolytes", Springer Nature, 2014 Publication	<1 %
46	Lei Zhang, Yiqun Liu, Yanxiang Zhang, Guoliang Xiao, Fanglin Chen, Changrong Xia. "Enhancement in surface exchange coefficient and electrochemical performance of Sr2Fe1.5Mo0.5O6 electrodes by Ce0.8Sm0.2O1.9 nanoparticles", Electrochemistry Communications, 2011 Publication	<1 %
47	Ting Kang, Bei Li, Qinglan Hao, Weijie Gao, Feng Bin, Kwun Nam Hui, Dong Fu, Baojuan Dou. " Efficient Hydrogen Peroxide (H O) Synthesis by CaSnO Two-Electron Water Oxidation Reaction ", ACS Sustainable Chemistry & Engineering, 2020 Publication	<1 %

48	Yan, A.. "Investigation of a Ba"0"."5Sr"0"."5Co"0"."8Fe"0"."2O"3"-"@d based cathode IT-SOFC", Applied Catalysis B, Environmental, 20060620 Publication	<1 %
49	booksc.org Internet Source	<1 %
50	derpharmachemica.com Internet Source	<1 %
51	digital.csic.es Internet Source	<1 %
52	gyan.iitg.ernet.in Internet Source	<1 %
53	hdl.handle.net Internet Source	<1 %
54	notablesdelaciencia.conicet.gov.ar Internet Source	<1 %
55	repositorio.ipen.br Internet Source	<1 %
56	repository.nwu.ac.za Internet Source	<1 %
57	www.annualreviews.org Internet Source	<1 %
58	www.tesisenred.net Internet Source	<1 %

59	www.x-mol.com Internet Source	<1%
60	Shenzhen Xu, Ryan Jacobs, Dane Morgan. " Factors Controlling Oxygen Interstitial Diffusion in the Ruddlesden–Popper Oxide La Sr NiO ", Chemistry of Materials, 2018 Publication	<1%
61	Wenqian Chen. "Engineering solid oxide fuel cell materials", Elsevier BV, 2020 Publication	<1%
62	Xuefeng Zhu, Weishen Yang. "Chapter 6 Perovskite-Type MIEC Membranes", Springer Science and Business Media LLC, 2017 Publication	<1%
63	Gu, H.. "Effect of Co doping on the properties of Sr"0"."8Ce"0"."2MnO"3"-"@d cathode for intermediate-temperature solid-oxide fuel cells", International Journal of Hydrogen Energy, 200809 Publication	<1%

Exclude quotes	Off	Exclude matches	Off
Exclude bibliography	On		